Effects of latitudinally heterogeneous buoyancy flux conditions at the inner boundary on MHD dynamos in a rotating spherical shell

Youhei Sasaki[1], Shin-ichi Takehiro[2*], Seiya Nishizawa[3] Yoshi-Yuki Hayashi[4]

[1] Department of Mathematics, Kyoto University, Japan, [2] Research Institute for Mathematical Sciences, Kyoto University, Japan,
[3] RIKEN Advanced Institute for Computational Science, Kobe, Japan, [4] Center for Planetary Science, Kobe University, Japan.
*contact: takepiro@gfd-dennou.org

Introduction

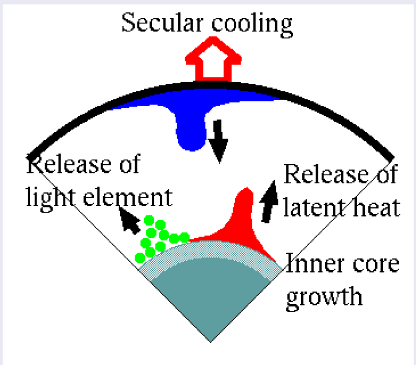

A schematic picture of the core dynamics

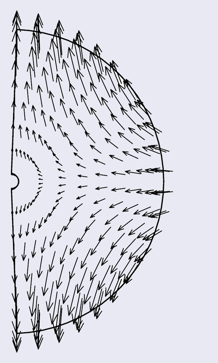

An example of inner core flows (Takehiro 2011)

- Outer core flows, contributing to generation and maintenance of the intrinsic magnetic field of the earth, is considered to be driven by buoyancy caused by the light elements released at the inner core boundary (ICB) through selective condensation of iron and nickel along with the inner core growth.
- On the other hand, existence of inner core flows has come to be studied as a candidate of the origin of the anisotropy of seismic velocity in the inner core. (Karato, 1999; Yoshida et al., 1996; Takehiro, 2011).
- The typical flow pattern expected in the inner core is axisymmetric and flows are directed from the equatorial region to the polar regions or vice versa.
- Since such a flow accompanies mass flux through the ICB, it affects the condensation process of iron and nickel, and as a result, latitudinal heterogeneity of the buoyancy (light elements) flux is expected to occur at the ICB.
- In the present study, **we investigate effects of latitudinally heterogeneous buoyancy flux at the ICB on dynamo process** in the outer core through numerical experiments of a 3-dimensional rotating spherical MHD Boussinesq dynamo model.

Model

- System: Boussinesq MHD fluid in a rotating spherical shell

$$\nabla\cdot\mathbf{u} = 0, \quad \nabla\cdot\mathbf{B} = 0,$$

$$E\left(\frac{\partial\mathbf{u}}{\partial t} + \mathbf{u}\cdot\nabla\mathbf{u} - \nabla^2\mathbf{u}\right) + 2\mathbf{e}_z\times\mathbf{u} + \nabla P = Ra\frac{\mathbf{r}}{r_o}\xi + \frac{1}{Pm}(\nabla\times\mathbf{B})\times\mathbf{B},$$

$$\frac{\partial\mathbf{B}}{\partial t} = \nabla\times(\mathbf{u}\times\mathbf{B}) + \frac{1}{Pm}\nabla^2\mathbf{B},$$

$$\frac{\partial\xi}{\partial t} + \mathbf{u}\cdot\nabla\xi = \frac{1}{Pr}\nabla^2\xi - 1.$$

- Variables:
  $\mathbf{u}$: velocity, $\mathbf{B}$: magnetic field,
  ξ : concentration of light elements.

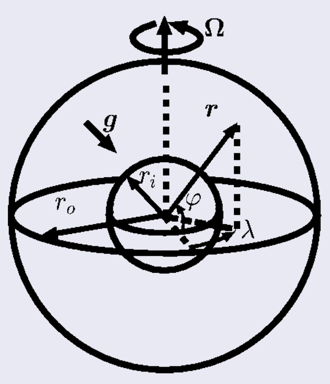

- Parameters:
  - the modified Rayleigh number: Ra
  - the Ekman number: E
  - the Prandtl number: Pr
  - the magnetic Prandtl number: Pm
  - The ratio of inner and outer radii
- Boundary conditions:
  - No-slip dynamical boundary condition
  - No compositional buoyancy flux at the outer boundary. Latitudinally buoyancy flux is given at the inner boundary.
  - The inner core is electrically conducting, allowed to rotate in a different angular velocity around the same rotation axis of the outer sphere.
  - The outside the spherical shell is electrical insulators.

Experimental setup

- Latitudinally varying buoyancy (light element) flux distribution:

$$F_i(\varphi) = -(1/Pr)\partial\xi/\partial r = F_0[1+\varepsilon P_2^0(\varphi)] = F_0\left[1+\varepsilon\frac{1}{2}(3\sin^2\varphi - 1)\right],$$

where $F_0 = (1/3)(r_o^3 - r_i^3)/(r_i^2)$.

- We consider the following three cases:
  - **Homogeneous distribution ($\varepsilon = 0$)**
    ⟵ no inner core flow.
  - **Strong flux around the equatorial region** and weak flux around the polar regions ($\varepsilon = -1$)
    ⟵ inner core flow is directed from equatorial to polar regions.
  - **Strong flux around the polar regions** and weak flux around the equatorial region ($\varepsilon = 2$)
    ⟵ inner core flow is directed from polar to equatorial regions.

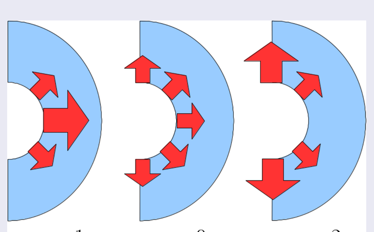

- Non-dimensional numbers
  - the modified Rayleigh number: Ra – varied from 100 to 500.
  - the Ekman number: $E = 10^{-3}$ (fixed)
  - the Prandtl number: $Pr = 1$ (fixed)
  - the magnetic Prandtl number: Pm – varied from 1 to 10
  - The ratio of inner and outer radii = 0.35 (fixed)
- Procedure
  - Firstly, numerical time integrations of purely compositional convection are performed starting with a point wise disturbance of light element concentration.
  - After statistical equilibrium states are established, MHD dynamo calculations are performed by adding dipole magnetic field.

Numerical methods

- Traditional spectral transform method.
- The temperature and the toroidal/poloidal potentials of $\mathbf{u}$ and $\mathbf{B}$ are expanded with spherical harmonic functions in the horizontal directions, Chebyshev polynomials in the radial direction of the shell, and the polynomials developed by Matsushima and Marcus (1994) in the radial direction of the inner sphere. .
- The time integration is performed with the Crank-Nicolson scheme for the diffusion terms and with the second order Adams-Bashforth scheme for the other terms.
- Resolution
  - The spatial resolution of the model is 128, 64, 32, and 24 grid points in longitudinal, latitudinal, and radial directions in the shell and the inner sphere, respectively.
  - Spherical harmonics, Chebyshev polynomials and the polynomials by Matsushima and Marcus are calculated up to the 42nd, 32nd, and 47th degrees, respectively.

Results of non-magnetic convection

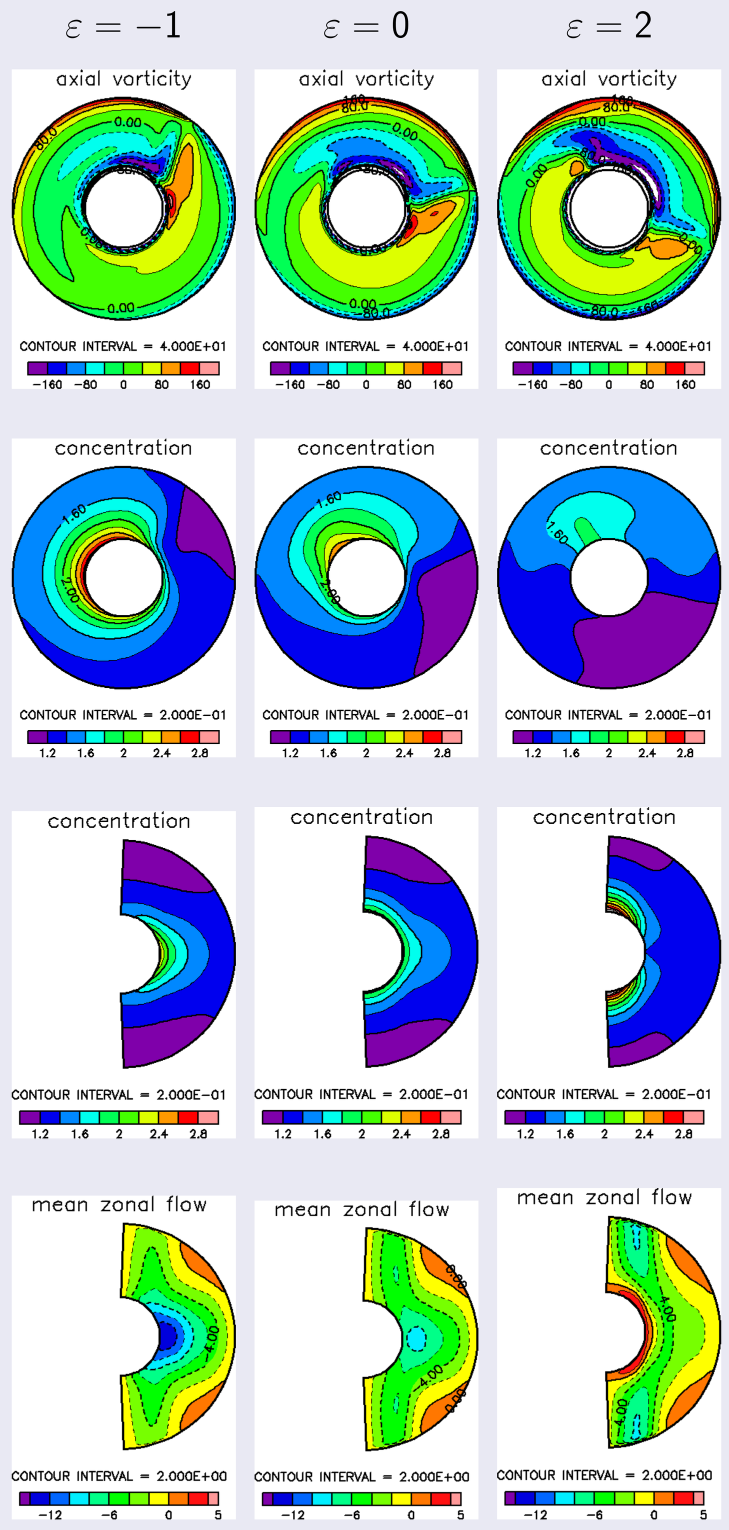

Figure (1) Structures of fully developed compositional convection without magnetic field for $Ra = 100$ and $Pr = 1$. Left, center and right columns shows the cases with $\varepsilon = -1, 0$ and 2, respectively. The first and second rows illustrate the axial vorticity and concentration of the light component fields on the equatorial cross section, respectively. The third and fourth rows denote the zonal mean concentration and flows in a meridional plane, respectively.

- Longitudinally elongated convective motion with longitudinal wavenumber one occurs.
- The difference between the values of ε in the zonal light element fields.
  - $\varepsilon = -1$:
    The light element distribution concentrates around the equatorial surface.
  - $\varepsilon = 0$:
    The light element distribution extends to the high-latitudes.
  - $\varepsilon = 2$.
    The light element distribution completely concentrates around the inner boundary.
- The difference between the values of ε in the mean zonal flow fields.
  - $\varepsilon = -1$:
    Strong retrograde flow concentrates around the equatorial inner boundary. The inner sphere rotates in the retrograde direction.
  - $\varepsilon = 0$:
    The zonal flow distribution extends outward. The inner sphere rotates in the retrograde direction.
  - $\varepsilon = 2$:
    Strong retrograde zonal flow emerges in the polar regions, while prograde zonal flows near the inner boundary rotates the inner sphere in the prograde direction.

Results of MHD dynamo experiments

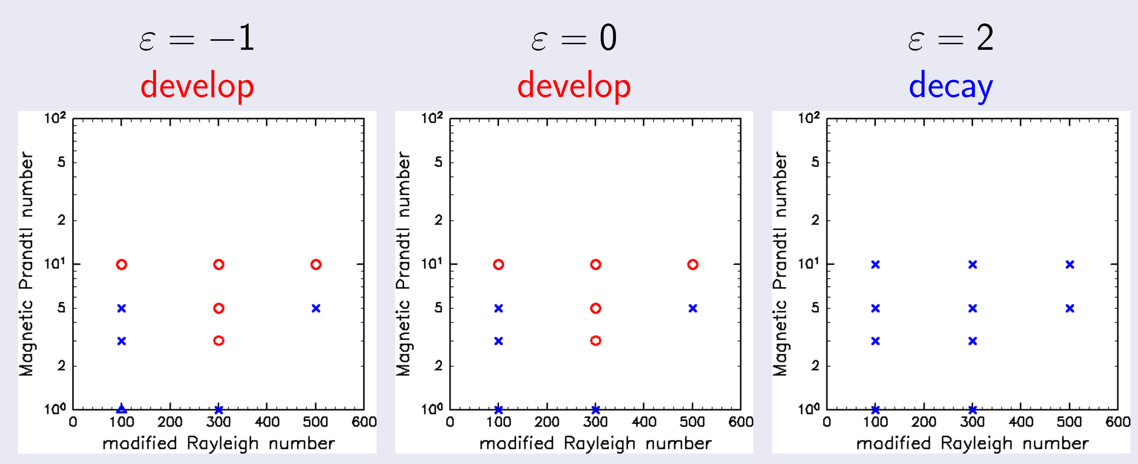

Figure (2) Diagrams of the experimental results for the MHD dynamo calculations. A blue cross denotes that a self-sustained dynamo solution does not develop. A red circle indicates that a dynamo solution develops.

- $\varepsilon = 0, -1$:
  The solutions where the magnetic field simultaneously develops and maintains (dynamo solutions) are obtained.
- $\varepsilon = 2$:
  The successful dynamo solutions are not obtained.
- $\varepsilon = 0, -1$ The dynamos develop most easily at $Ra = 300$, and the successful solutions are obtained when $Pm \geq 3$. Establishment of the dynamo solutions becomes difficult when the Rayleigh number is either increased or decreased.

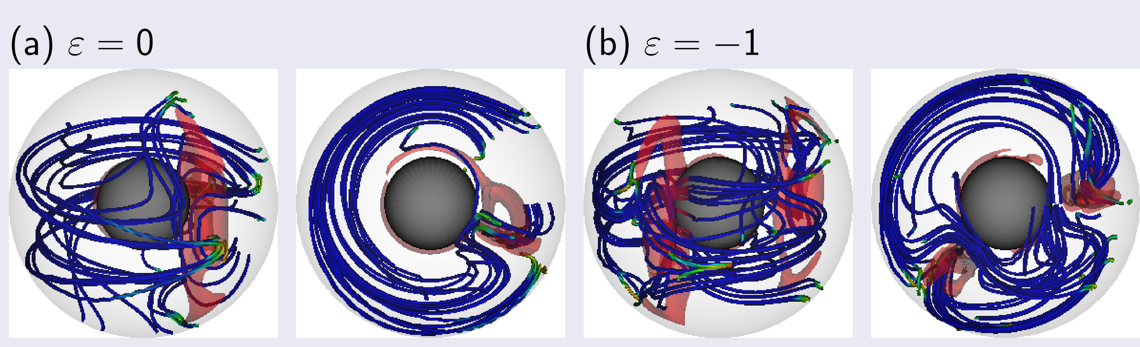

Figure (3) 3-dimensional plots of the magnetic field lines and vortex surface for $Ra = 100$, $Pm = 10$. The upper panels are the case with $\varepsilon = 0$. The lower panels are the case with $\varepsilon = -1$. The left panels observe from a mid-latitude and the right panels is from the north pole.

- The toroidal magnetic field around the equatorial surface is lifted up in the polar directions and twisted at the western side of the concentrated anti-cyclonic vortex tube, causing the poloidal magnetic field generation.
- The poloidal magnetic field is wound from the eastern to western sides of the vortex tube by the anti-cyclonic vortex motion, and the toroidal magnetic field is generated.
- Positive feedback of these generation mechanisms of the toroidal and poloidal magnetic fields is considered to maintain the magnetic field.

Experiment with buoyancy boundary condition switching

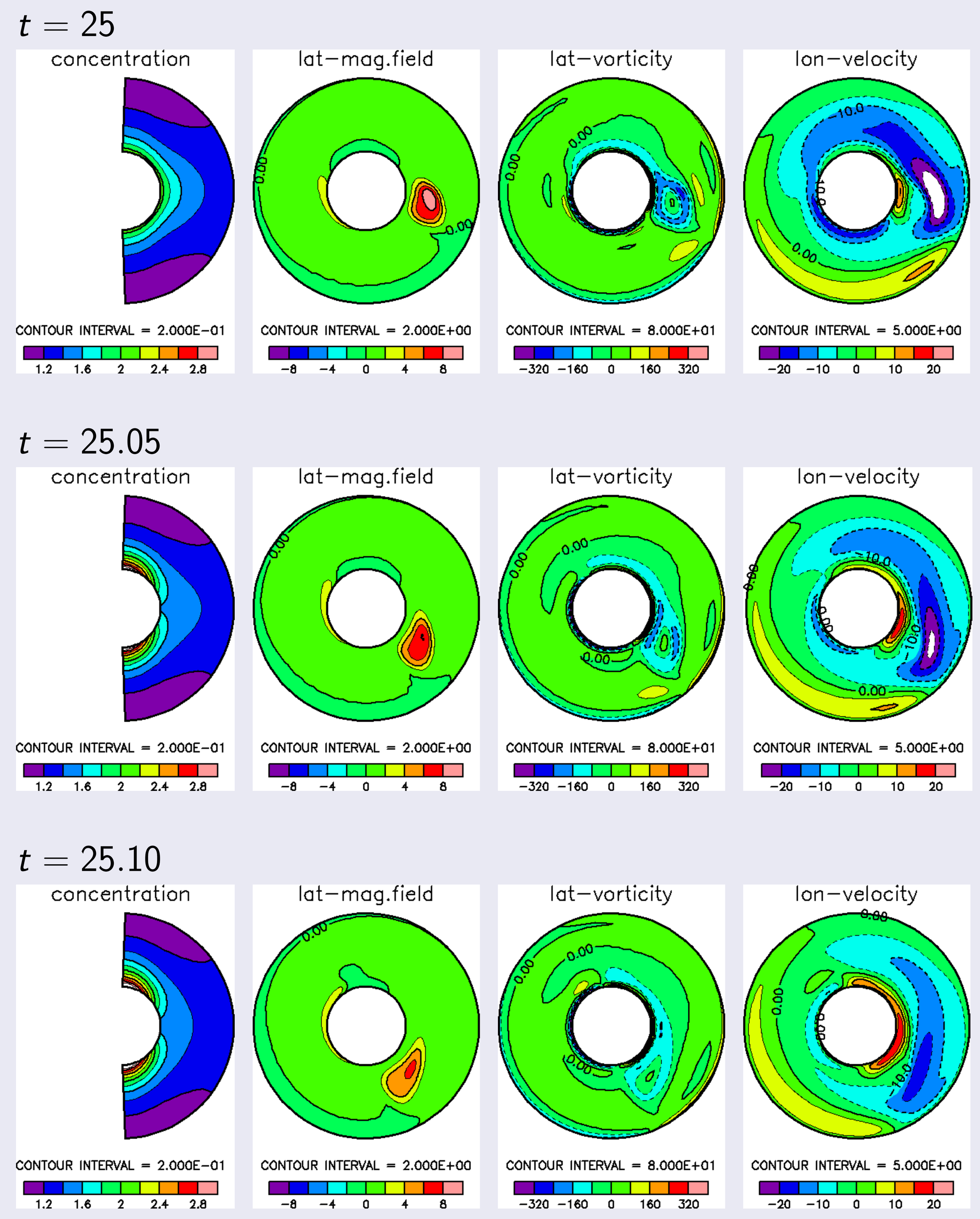

Figure (4) Time development of the experiment where the buoyancy flux boundary condition of the self-sustained dynamo solution obtained when $\varepsilon = 0$ (Figure 3a) is changed to $\varepsilon = 2$ instantaneously. From the left to right columns, zonal mean light element concentration, axial magnetic field and vorticity in the equatorial cross section, and mean zonal flow are shown, respectively. The top panels are the dynamo solution at $t = 25$ when $Ra = 100$, $Pm = 10$, and $\varepsilon = 0$. Time development of each field after the change of the boundary condition is shown in the middle ($t = 25.05$) and bottom ($t = 25.1$) panels.

- In order to examine the reason why no self-sustained dynamo solution develops in the case of $\varepsilon = 2$, we perform the additional experiment where the buoyancy flux boundary condition of the self-sustained dynamo solution obtained when $\varepsilon = 0$ (Figure 3a) is changed to $\varepsilon = 2$ instantaneously.
- One concentrated anti-cyclonic vortex and the associated magnetic flux tube are weakened.
- This disruption of the vortex and magnetic tubes is considered to be caused by the prograde flow along the surface of the inner sphere (4th column of Figure 4).
- The strong shear associated with the zonal flow seems to drag and elongate the vortex tube, causing the stretching and weakening of magnetic flux tube.

Discussions

- Numerical experiments of compositional convection and MHD dynamo in a rotating spherical shell are performed with strong equatorial buoyancy flux ($\varepsilon = -1$), strong polar buoyancy flux ($\varepsilon = 2$), and homogeneous buoyancy flux conditions ($\varepsilon = 0$).
- There are little differences in flow fields of fully developed purely compositional convection except for the distribution of mean zonal flows.
- In the MHD dynamo calculations, different developments of the magnetic field are observed according to the distribution of buoyancy flux at the inner boundary.
  - When the homogeneous buoyancy flux is given ($\varepsilon = 0$) or strong flux is given around the equatorial region ($\varepsilon = -1$), self-sustained dynamo solutions are obtained for sufficiently large magnetic Prandtl numbers.
  - However, when strong flux is given around the polar region ($\varepsilon = 2$), all solutions are failed to sustain the magnetic fields in the surveyed ranges of the parameters.
- This difference in development of magnetic fields is considered to be affected by the different pattern of mean zonal flow.
  - In the case of strong polar buoyancy flux, direction of mean zonal flow around the inner core is reverse through the thermal wind balance and strong shear layer is produced there.
  - This shear may stretch the convection columns and prevent localization of the vortex columns and magnetic field.
- Geophysical implications:
  - It may not be expected that the inner core flows is directed from the polar regions to the equatorial region, because such a buoyancy flux pattern may be unfavorable for development and maintenance of the strong geomagnetic field.
  - Further investigation in more broad ranges of the parameter space is needed, since the values of the parameters dealt with the present study are quite different from those of the real central core of the earth.

Acknowledgments

- The library for spectral transform 'ISPACK' (http://www.gfd-dennou.org/library/ispack/) and it's Fortran90 wrapper library 'SPMODEL library' (http://www.gfd-dennou.org/library/spmodel/) were used for the numerical calculations.
- The numerical codes used in the present study is also available from the 'SPMODEL MHD Dynamo' web site: http://www.gfd-dennou.org/library/dynamo/
- The products of the Dennou-Ruby project were used to draw the figures: http://www.gfd-dennou.org/library/ruby/

References

- Karato, S., "Seismic anisotropy of the Earth's inner core resulting from flow induced by Maxwell stresses", Nature, 402 (1999), 871–873.
- Yoshida, S., Sumita, I., Kumazawa, M., "Growth model of the inner core coupled with the outer core dynamics and the resulting elastic anisotropy", J. Geophys. Res., 101 (1996), 28085–28103.
- Takehiro, S., "Fluid motions induced by horizontally heterogeneous Joule heating in the Earth's inner core", Phys. Earth Planet. Inter., 184 (2011), 134–142.
- Matsushima, T., Marcus, P. S., "A spectral method for polar coordinates", J. Comp. Phys., 120 (1994), 365–374
- Takehiro, S., Odaka, M., Ishioka, K., Ishiwatari, M., Hayashi Y.-Y. and SPMODEL Development Group, A series of hierarchical spectral models for geophysical fluid dynamics, *Nagare Multimedia* 2006, Available online at: http://www.nagare.or.jp/mm/2006/spmodel/